TRACTION IN WEB HANDLING: A REVIEW

by

D. P. Jones
Emral Ltd.
UK

ABSTRACT

In web processes, at least one moving machine component must drive the material through a friction force at the interface. This force, or traction, inevitably falls as speed increases, and is accompanied by a degree of slip. As a result, traction often limits productivity through constraints on product output and quality. Although there are high traction elements available for web lines, such as nips, edge grippers and vacuum pull rollers; the majority of machines still rely on driven rollers wrapped by the web. Machinery manufacturers seek to optimise the design of the traction elements by specifying layout, drive and roller surfaces, whereas material manufacturers seek web surfaces that will perform well irrespective of machine. In other situations, low traction may be desirable. A roller imparts stability to the web if traction is high enough to ensure speed matching, or if the traction is low at all times so that roller has little influence on the web. It is important to avoid intermediate situations where intermittent slip occurs.

An understanding of traction, and design tools based on validated models, are clearly desirable. The reduction in traction with speed is dependent on roughness of web and roller. Current models tend to be based on statistical descriptions of the surfaces, rather than parameters suggested from the physics of the interaction. However, the models do permit a number of subtle effects, such as web permeability and the constriction at the exit point, to be included.

When applying traction theory to a web line, it is important to know where the web and roller speeds are matched, and this cannot be designated arbitrarily. Furthermore, adjustments of one roller speed can result in a remote roller moving from speed matched to a slip situation. A model, validated at low speeds, will be used to demonstrate these effects.

Traction also provides force perpendicular to the direction of web travel. Loss of traction may occur if the vector sum of lateral force and tension change is greater than the available friction force, causing web movement sideways. Also, lateral traction and slip are important in determining wrinkling and scratching on a roller.

Deviations from elastic web behaviour reduce available traction. The areas of speed matching no longer have constant tension, and extra zones of slip may appear. As an example, a model of a thermal vapour deposition on a film on a cooled drum will be described. The heat load causes thermal expansion, which tends to reduce tension in the machine direction and generate lateral compression. If the tension is too low, wrinkles form, and are set in as the material lifts off the drum and rapidly heats up.

NOMENCLATURE

e	The base of natural logarithms, 2.718
E	Young's modulus of the web
f	Parameter in equation {9} between 1.67 and 3.09, but dependent on other variables
F	Reaction force set up by web bending
G	Torque per unit width applied to roller
h	Gap between web and roller surfaces
h_0	Entrained air layer thickness between smooth web and roller, equation {4}
h_1	Constant value of surface separation in fixed gap model
M	Reaction bending moment set up by web bending
MD	Machine Direction, i.e. along direction of travel
p_a	Pressure of air entrained between web and roller
p_c	Sum of forces on actual contact points between web and roller per unit area
PTFE	Poly(tetrafluoroethylene)
R	Roller radius
R_a	Mean value of the average roughnesses of web and roller surfaces
R_q	Square root of the sum of the mean square roughnesses of web and roller surfaces
t	Web thickness
T	Web tension (force per unit width)
T_1	Entry tension
T_2	Exit tension
TD	Transverse Direction, i.e. perpendicular to direction of travel
v	Speed
v_1	Web speed on entry
v_2	Roller surface speed
w	Web width
ΔT	Increase in web tension over a roller
Δv	Increase in web speed over a roller
η	Dynamic viscosity of air
θ	Angle of wrap
μ	Coefficient of friction
μ_T	Coefficient of traction, defined in equation {5}
ρ	Web mass per unit area
σ	Stress
σ_{crit}	Critical value of compressive stress for buckling
σ_y	Transverse direction compressive stress
$\sigma_{y\,max}$	Maximum value of transverse direction compressive stress

INTRODUCTION

The term *traction* has come into use for web handling systems to describe the degree of grip or slip between the web and other surfaces, normally rollers. Classical friction concepts need extending to describe the behaviour as the speed is increased. Although there is a recognised distinction between static and dynamic friction, with the surfaces in relative motion in the latter case, traction describes the situation where at least one of the surfaces is moving at high speed and the contact pressure is low, so that air entrained by the moving surfaces bears a significant fraction of the nominal contact pressure, and the apparent coefficient of friction is reduced. Although the surfaces may be moving at speeds of 1 m/s or more, their relative velocity may be very small or even zero.

Traction effects are encountered in many everyday situations, for example automobile tyres. The tread may not be deep enough to penetrate a water puddle on the road, in which case traction is lost and any attempt to change velocity such as steering or braking is ineffective. Even without fluid, traction limits the maximum force that can be applied to the road surface. Attempts to apply a higher force result in a speed differential and a skid or wheel spin.

In web handling machinery, good traction is needed for several reasons:

- To maintain different levels of tension in each section of the machine, for example, unwind, coating, drying and rewind.
- To avoid uncontrolled lateral web movement, which may change the position of the web relative to slitting blades, coating devices, heaters and the rewind core. Making allowance for this by decreasing the usable portion of the width reduces productivity.
- To maintain the web taut during machine start, stop and speed change operations.
- To reduce the propagation of tension disturbances by coupling the web to the inertia and damping of rollers.
- To enable spreading devices to pull the web taut.
- To enable steering guides to control the lateral web position.
- To minimise scratching and scuffing.
- To enable higher speeds before these problems become apparent, and hence increase productivity.

For reasons of cost and simplicity, rollers are the most common web line elements. Most of this paper will address web traction on rollers. However, their traction performance is limited, and elements with much higher traction are available, but at a cost.

In other instances, minimal traction is required whilst the web is supported, for example in dryers and around air turn bars. Scratching and other web damage can be reduced, and web position is virtually unaffected as the force applied is very low.

This paper gives a review of published work on traction of webs on rollers. The first section outlines the basic mechanics of a web on a roller, and the incorporation of air entrainment effects by analogy with the foil bearing. Models developed to relate traction test data and surface roughness to web handling equipment are assessed for accuracy, practicality and usefulness. The second section considers traction through a line with several elements, and some data obtained on a production slitter-rewinder are analysed.

The next section describes lateral effects of traction, in steering, wrinkling and scratching. Finally, the case of non-elastic webs is considered, and a model for wrinkling of a web under high heat load on a vacuum coater drum presented as an example.

WEB ON A ROLLER

Basic Mechanics

Figure 1 shows the simple situation of a flexible web passing over a rigid driven roller, radius R. In steady state, the web tension difference (T_1-T_2) must balance the torque per unit width G applied to the roller, regardless of the state of slip at the interface:

$$T_1-T_2 = G/R \qquad \{1\}$$

The tension ratio can take any value from 1 up to that given by the *belt equation* (also known as the capstan or Eytelwein equation):

$$T_1/T_2 = e^{\mu\theta} \qquad \{2\}$$

where μ is the coefficient of friction and θ the angle of wrap in radians. When the ratio is 1, no torque is transmitted and the web and roller surface speeds are matched over the whole arc of contact.

As the torque increases, the speeds are still matched over the first part of the contact, but the tension change occurs in a *microslip zone* in the last part (figure 2). In this zone, the web gradually contracts elastically, and moves relative to the roller surface. This is analogous to belt creep on the drive pulley in a flat belt drive. For the case of a roller that is braked or idling with bearing friction, the same equations {1} and {2} apply, with the suffices 1 and 2 exchanged; the web now extends in the microslip zone.

The tension gradient at any point along the contact can take one of two values: either zero with zero slip velocity, or a value equal to the friction coefficient times the normal force, i.e.

$$dT = 0 \text{ or } \frac{dT}{Rd\theta} = -\mu\frac{T}{R} \qquad \{3\}$$

Integrating {3} gives equation {2}. Force equilibrium can be satisfied in principle with the microslip zone located over any part of the wrap. However, this zone will travel with the web movement around the roller. The only stable condition has the microslip zone at the exit with the tension in the following free span providing a boundary value.

If the tensions or torque vary with time, there may be a microslip zone at the entry, and sections with a tension gradient are propagated around the roller [1].

Air Entrainment

The earliest reference to the inadequacy of the belt equation appears to be Daly's paper in 1965 [2]. Traction was quantified by the maximum torque transmitted by a moving paper web to a braked smooth steel roller. As expected, traction increased with web tension and angle of wrap. However, it fell with increasing speed and decreasing paper permeability. This progressive loss of traction was attributed to air entrainment, with the web eventually attaining a fully floating condition. With high porosity papers, air was able to escape through the web and traction was maintained virtually unchanged up to 20 m/s.

Knox and Sweeney [3] carried out traction experiments on polyester films, and applied fluid dynamics results for the foil bearing, which consists of a rotating shaft supported by a stationary flexible foil with a lubricating air layer [4]. In web handling, both web and roller are normally moving as they converge. The air layer entrained by the

smooth impermeable web and roller surfaces shown in figure 3 has constant thickness over most of the angle of wrap, given by [5]:

$$h_0 = 0.643R\left(\frac{6\eta(v_1 + v_2)}{T_1}\right)^{2/3} \qquad \{4\}$$

where η is the viscosity of air (18.5×10^{-6} Pa s), v_1 and v_2 are the surface speeds of the web and roller respectively, and T_1 is the entry tension. For example, a web coming onto a 0.125 m radius roller (10 in. diameter) at 5 m/s (1000 ft/min) and 100 N/m (0.6 pli) tension will entrain a 40 μm air layer. The air pressure, given by T/R, is 0.8 kPa (0.11 psi). Knox and Sweeney demonstrated that if h_0 is much higher than the peak heights making up the web surface roughness, the traction is very low, whereas if h_0 is small, traction is unaffected by entrained air, and can be predicted from the coefficient of friction. Jones [6] reported similar results, confirming higher traction from rougher webs.

Predicting Traction

Subsequent work has recognised that the roughness of both surfaces contributes to the traction. Ducotey and Good [7,8] have carried out extensive traction measurements as a function of roller diameter, wrap angle, surface composition and roughness, tension and speed for different web materials. They increased the braking torque on a roller until its speed fell below that of the web. They then calculated a *coefficient of traction*, μ_T, from the experimental data, using a modified form of equation {2}:

$$T_2/T_1 = e^{\mu_T\theta} \qquad \{5\}$$

Plotting μ_T against the calculated air layer thickness for smooth surfaces, h_0, a single curve results from different tensions, diameters and angles of wrap. Changing surface roughness gives a different curve. They developed an algorithm for μ_T:

$$\mu_T = \mu \text{ for } h_0 < R_a$$
$$\mu_T = \mu\frac{(3R_q - h_0)}{(3R_q - R_a)} \text{ for } R_a < h_0 < 3R_q \qquad \{6\}$$
$$\mu_T = 0 \text{ for } h_0 > 3R_q$$

where R_a is the mean of the average roughnesses of the two surfaces, and R_q is the combined root mean square roughness.

At low speeds, the coefficient of traction is equal to the coefficient of friction μ, which Ducotey and Good assumed to be the static coefficient [8]. For a metal roller, the dynamic coefficient is more appropriate: there is a static friction force with no relative movement only on the line separating the stick and microslip zones, and virtually all the tension change occurs over the microslip zone where the two surfaces are in relative motion. For a roller with a compliant rubber covering, the static coefficient may be preferable, as shear in the rubber can take up the change in web strain [9]. If a laboratory measurement of coefficient of friction is used to predict traction, it should be taken under applicable conditions, particularly very low sliding speed and normal pressures of order 1 kPa.

The existence of a region of constant μ_T at low speed appears to have been surmised from one curve presented by Knox and Sweeney [3]. No other experimental dataset contains points at low enough speed to confirm its existence. The modelling results described below suggest a continuous decrease is the likely behaviour. Further experimental studies in this area would be useful.

The use of the average surface roughness parameters is also questionable. R_a and R_q contain the whole range of surface heights, and are unlikely to describe accurately the very highest surface peaks in contact. Surface textures of machined metal roller surfaces, plastic film and paper are very different in character, so the relationship of the maximum peak heights to the statistical averages will not be the same. Similarly, the combination of two different surfaces is unlikely to behave like those in lubricated metal bearings.

The use of equation {5} is only an approximation, as shown below. As a result, the coefficient of traction is not truly constant and will vary with the other variables, including wrap angle.

The simple fit in equation {6} predicts too low a traction at high h_0, either because regions of higher contact pressure at the web edges and exit persist at high speed, or because of the distribution of peak heights.

Despite these shortcomings, the coefficient of traction approach does provide a prediction of traction which can be applied in a familiar way, and it can be calculated from measurements of surface roughness and coefficient of friction for any value of diameter, wrap angle, speed and tension. For design and troubleshooting of web lines, the required accuracy is low: it is sufficient to know the conditions under which traction is significantly reduced, say to 50% of its low speed value, and when the web is fully floating. The coefficient of traction algorithm is included in commercial computer software programs [10,11]

Possible Web Condition

To summarise, the web may be in one of four conditions on a roller:
- *Stick* with web and roller speeds matched over the whole contact, and hence no scratches. A tension change is only possible with a compliant roller covering.
- *Microslip* with a stick zone at the entry, and a microslip zone at the exit. There will be a tension change within the limits of equation {5}, speed matching at entry, and possibly very small scratches.
- *Slip* where there is no stick zone, and a tension change given by equation {5}. The speed difference can be large, and scratches are likely.
- *Floating* where the air layer is thick enough to prevent contact between the surfaces. The speed difference can be large but there will be zero tension change and no scratching.

The slip condition is clearly undesirable. The web is prone to lateral movement and scratching. Microslip close to the limit of equation {5} is also potentially damaging, as tension fluctuations or large lateral forces may take the web into the slip condition intermittently.

Contact Modelling

The detailed modelling of the web-roller interaction is of interest to web manufacturers who require good traction without a deterioration of other properties resulting from traction additives. For example, small amounts of inorganic filler are added to polyester before extrusion, which cause surface peaks after biaxial stretching (figure 4). However, they introduce haze, reduce gloss and sometimes the larger particles can be seen individually. Some surface roughness is required to prevent blocking, and

the surface topography also controls some aspects of roll quality through the compression behaviour of film layers [12]. A more sophisticated contact model may enable traction and the other properties to be optimised together. For example, a filler recipe that produces the high surface peaks for traction but reduces the haze and the mean surface roughness may be desirable.

Figure 5 represents schematically the forces acting on an element of the web on the roller. The component of tension acting inwards balances air pressure in the gap, a true normal contact force on the surface peaks, and the centrifugal force:

$$\frac{T}{R} = p_a + p_c + \frac{\rho v_1^2}{R} \qquad \{7\}$$

The centrifugal force is proportional to web mass per unit area ρ, and is only significant at very high speeds. The air pressure p_a arises from the converging flow prior to entry. Only the contact pressure on the surface peaks p_c can generate a friction force, resulting in a tension gradient analogous to equation {3}, if sliding occurs:

$$\frac{dT}{Rd\theta} = \mu p_c \qquad \{8\}$$

A key feature of the contact is the dependence of the contact pressure on surface separation, $p_c(h)$. It is possible to measure this directly [3,13], at least when the surfaces are fairly smooth, but most authors have assumed a functional dependence. The simplest assumption is that the surfaces are either out of contact or they have a fixed separation h_1 with surface peaks or asperities in contact [6,14]. In modelling recording head-tape contacts, Wu and Talke [13] found their directly measured curve fitted both the Greenwood and Williamson contact model [15] and a parabolic curve well. Rice et al. [16] also used the parabolic curve, with an asperity engagement height and asperity compliance obtained by fitting the traction data. They showed that the asperity compliance has little effect on the results: the main effect of an increase in contact pressure is to bring more asperities into contact. They provided a prescription for estimating the asperity engagement height from surface roughness parameters, which took into account the importance of high peaks on both surfaces.

Unfortunately, the roughness parameters chosen are dependent on the sampled surface area: the larger it is, the more high peaks will be found. An approach that uncovers the underlying distribution of peak heights should be preferable: however this requires a large area to be sampled in order to reduce the statistical uncertainty. There may be only one peak in an area of 1 mm^2 making contact between web and roller. The typical sampling area of a profilometer is smaller than this; so many samples must be taken. It would then be possible to use standard contact mechanics theory [17] to calculate $p_c(h)$ with no undetermined parameters. Greenwood and Williamson use a specific Gaussian distribution curve [15], but this may not represent all surfaces well.

This approach would also give a clear method to combine two surfaces. Since the compliance of a rigid asperity pressing into a compliant flat surface is identical to that of a compliant asperity pressing against a rigid surface, and the contacting asperities are so widely spaced that they are unlikely to interact, the peak height distributions for the two surfaces should be simply added together.

Further refinement of the approach will be necessary when the web is thin (below 100 μm), as it will bend between points of contact [18].

193

To determine the air pressure in the gap, p_a, the entry region must be modelled. The balance of forces on the web is represented by equation {7}, with the roller radius replaced by the local radius of curvature of the web. Air flow is modelled by the Reynolds Lubrication equation, which needs to include slip flow effects if the gap is smaller than a few times the molecular mean free path (0.1 μm) [16,19]. It is generally assumed that the effective surface separation for flow is the same as for contact, and the presence of roughness does not perturb the flow. These potential corrections have been studied in magnetic tape-head contacts [20] but not applied to web traction. Compressibility effects should be negligible unless T/R is greater than 12 kPa [21], but appear to be more significant than this in the model of Schüler et al. [14].

The exit region of the foil bearing contains a region of reduced gap and air pressure [5]: the corollary of this when contact occurs is an increase in the contact pressure p_c and hence an area of locally increased traction.

The numerical models of Rice et al. [16] and Schüler et al. [14] both compute the traction over the whole contact (showing the exit effect). Rice et al. show good agreement with experimental data for 8 webs on the same roller, albeit with some fitted parameters as described above.

The modelling studies contain additional sophistication, which is important in some cases. Rice et al. [16] include web stiffness effects. Traction is greater for permeable webs and when side leakage occurs, as the air pressure falls along the contact [8,22]. By comparison with the foil bearing [23], there may be an enhancement of traction at the web edges, as the air pressure falls to zero at the edge and therefore the contact pressure is increased. This effect will be especially significant at high speeds: when contact has been lost over the main part of the wrap angle, the reduced pressure regions at the edges and exit region may still provide traction.

Simple Analysis of Traction Tests

If the analysis outlined above is simplified, the behaviour of the web-roller system can be predicted without recourse to numerical analysis. Traction is assumed to arise solely from the main part of the contact, ignoring entry, exit and edge regions.

The air pressure p_a can be estimated for the constant gap model using:

$$p_a = \frac{f\eta(v_1 + v_2)}{h_1^2}\sqrt{Rh_1} \qquad \{9\}$$

The parameter f takes the value 1.67 if the web remains straight coming onto the roll [6], and 3.09 if it is just on the point of touching the asperities [14]. For other cases, the numerical integration must be carried out. Substituting equation {7} into {8} gives a modified belt equation:

$$\frac{T_1 - p_a R}{T_2 - p_a R} = e^{\mu\theta} \qquad \{10\}$$

This differs from equation {6}: hence the coefficient of traction can now be seen to be only an approximation.

In addition to the experiments mentioned above, Ries and Farr [24] have measured the velocity of a braked roller as a function of torque for different surfaces, speeds, tensions and wrap angles. They found that at torques greater than that required to initiate

194

slip, the idler roll was still turning but below web speed. This can be understood from lower entrained air pressure as a result of the lower roll speed increasing the contact pressure and hence the traction force [6]. Without air entrainment, the roll would be brought to rest by the critical torque.

This is illustrated in figure 6 by a simulation of the data in figure 6 of [24], with values 0.15 for coefficient of friction and 5 μm for the constant gap h_1, which is reasonable for the roller roughness of 1.5 μm. Film and roller speeds match up to the point of slippage, beyond which the speed difference increases with torque. The agreement between the data and the simulation is only qualitative, as the speed difference increases more steeply with torque in the simulation. This is possibly due to a reduction in the factor f in equation {9} as speed difference increases.

Increasing Traction

Ries and Farr [24] showed that the reduction in traction with speed could be virtually eliminated with a grooved or knurled roller. Traction from these surfaces has not yet been modelled. The web will be pulled into grooves and over knurl pips, giving regions of high traction. Only in the case of very fine grooves will the web remain cylindrical, in which case an equivalent depth for the air entrainment could be used in the theory for plain rollers [25].

Other ways to increase traction are to use rougher surfaces, increase tension and wrap angle, and decrease roller diameter, as predicted by the traction theory. The normal force on the contact can be increased by the use of nip rollers, vacuum pull rolls, electrostatic pinning, air knife assist, and suction assist, giving a major improvement in traction and removing most of the dependence on tension and diameter. A further interesting possibility is to use a "gap throttle foil" which reduces the air entrained [14].

TRACTION IN A SLITTTER-REWINDER

Very large slitter-rewinders for plastic films (up to 9 m wide) are frequently provided with individual drives on each roller. Their relative speed settings and traction determine the tension profile through the line. Some experiments were carried out by the author to demonstrate the effect of changing these settings.

Experimental Details

The main group of rollers is shown in figure 7. After the offwind, the film passes around free-running tendency driven rollers (not shown) and a dancer roller where the offwind tension was set to 135 N/m. The relative speed of the next roller (driven roller no. 1) was adjusted in the experiment. The driven rollers were rubber-covered with a coarse diamond groove pattern.

The dynamic coefficient of friction between film and roller was determined by hanging weights on one end of a strip of film draped over a roller, and measuring the force on the other with a spring balance while it was moved at a slow steady rate in either direction. The belt equation {2} was used to obtain a value of 0.4 from readings with different weights and at different locations along the roller length.

3.4 m wide, 12 μm thick polyester film was run through the machine at 0.5 m/s (30 m/min), then at 13 m/s (800 m/min).

The relative roller speeds were set using the machine computer control. Their diameters were measured, and their rotational speeds measured simultaneously using an optical multichannel counting interface on a PC. In this way, the relative surface speeds could be determined accurately even when the machine speed was drifting. There were

195

significant errors in the roller diameters assumed by the machine computer control, resulting in the actual relative speeds being different from the set values.

Tensions were measured in the indicated span by the "Tensor" hand-held sensor [26] at different relative speed settings. The offwind tension was calibrated using the spring balance, and then used to calibrate the Tensor at different tensions in the moving web. The average tension from 5 readings across the web was taken. Unfortunately, other spans were inaccessible so could not be measured.

Results

The measured tension results at 0.5 m/s, shown in figure 8, show considerable scatter, but follow the expected pattern. When driven roller no. 1 runs slower than the line, it is braking and the tension in the span following is high and independent of its speed. When it runs faster than the line, it is driving and the tension is low. The ratio of the two tensions agrees with that calculated from the angle of wrap and measured dynamic coefficient of friction.

When the roller runs close to line speed, the tension decreases linearly with roller speed. The film and roller speeds are matched on entry, but the increase in web speed Δv over the roller determines the tension change ΔT:

$$\Delta T = Et\frac{\Delta v}{v_1} \qquad \{11\}$$

The film exit speed is equal to the next roller speed (unless it is in the slip condition). If the roller speed is reduced, the speed change on the roller increases, and gives a higher tension in the exit span. The slope of the data in figure 8 in this region is correctly predicted from the film modulus E (4.5 GPa) and thickness t. The apparent roller speed at which the entry and exit tensions are equal is 0.11% slower than the machine speed indicated by the computer control. However, the true speed of the roller is actually 0.23% faster than that of the reference roller (no. 5)! This behaviour can be understood using a model described in the next section.

When the machine speed is increased to 13 m/s, the difference in tension between low and high relative roller speeds falls and cannot be untangled from the data scatter. An upper limit of 0.05 can be placed on the coefficient of traction.

Model for Roller Sequences

In the machine configuration tested, and probably in much other web handling equipment, the true roller speeds are set quite far apart. If equation $\{11\}$ is applied through the machine, starting with the known offwind tension and assuming that the web speed is equal to each roller speed at the entry point, a tension profile is obtained. However, the calculated tension ratio across some of the rollers may exceed the limiting value specified by equation $\{6\}$, and so the profile is in error. The procedure described by Zahlan and Jones [27] enables the profile to be calculated in these circumstances. It selects the correct roller on which the web entry speed and roller speed are matched: this is the first one in the sequence which gives tension changes from equation $\{11\}$ and tension ratios from equation $\{6\}$ on rollers which are slipping.

When applied to the slitter-rewinder data as shown in figure 8, it predicts that the roller 1 (see figure 7) moves from slipping at less than the web speed, through a region of speed matching, to slipping faster than the web speed as its speed is increased. The procedure correctly predicts the speed at the transitions between each regime. Roller 2 is

always slower than the web. The speeds are always matched on entry to roller 3. Roller 4 is always faster than the web as a result of a 1% error in the diameter value in the machine computer control. Roller 5 is designated as the "master speed roller", but moves from speed matched to underspeed as the speed of the first roller increases. An arbitrary designation of a "master speed roller" does not guarantee that its speed will set the web speed.

Further validation of this model would be desirable, and would be easier on a laboratory machine on which roller torques could be measured easily.

The model can be adapted for use for idler rollers, and for rollers driven together. The effect of speed and diameter deviations can be explored: quite small changes may give large tension changes on stiff webs such as polyester. In addition, the model can identify where slip and possible scratching of the web is occurring.

LATERAL EFFECTS

In addition to the machine direction (MD) effects, traction can influence the transverse direction (TD) behaviour of the web.

Steering

The principles of steering when the rollers are in either the stick or microslip condition are well known [28]. In steady state, the web comes onto the roller at right angles to the roller axis (*the Normal Entry Rule*) as a result of the web velocity matching the roller velocity over the stick zone. In the preceding free span, the web bends as a beam. An inclined roller therefore produces a lateral deflection of the web, and sets up a reaction force F on it together with a reaction force and moment M acting on the entry roller (see figure 9). The reaction forces and moment are transmitted through traction between the web and roller.

As the angle of inclination increases, eventually the forces or moment reach the limits imposed by traction. If the force limit is exceeded, the normal entry rule no longer holds and the web deflection is dependent on the traction forces. Lateral position is therefore influenced by machine speed, which reduces the traction, and by fluctuations in tension. If a stick zone is reestablished, the web will move back towards the normal entry position [28]. As a result, the web position can vary undesirably. Daly [2] reported observations of lateral web shift when rollers moved from stick to full slip behaviour, but stability if the stick condition or full slip condition was maintained throughout. Observations and quantitative measurements of lateral instability during winding have also been linked to traction [3,6].

The bending moment at the roller exit imposes a tension gradient across the web. The tension at each edge is limited by equation {6}. Once that limit is reached, slip occurs over the whole wrap for a portion of the film width, and a bending moment is imposed on the web entering that roller, although normal entry is preserved. This is termed *moment transfer*, and again changes the web deflection by an amount depending on traction [29,30,31].

Each roller may therefore have to support lateral forces and moments arising from both the entry and exit spans, and a machine direction force to balance the roller torque as in equation {1}. Traction limits the *resultant* of these forces. The consequence is that a roller on which the web tension changes significantly, is much more likely to lose traction in the lateral direction as the lateral force it can support is lower. Conversely, a misaligned roller will have less capacity to accommodate a tension change, as slip will occur before the limit of equation {6} is reached.

197

Wrinkling and Creasing

Thin webs often exhibit wrinkling or *troughing* in spans, caused by misalignment [32], Poisson's ratio expansion accompanying a tension fall on the entry roller, or convergence effects from the exit roller having a barrel shape or bending significantly under its own weight or applied forces [33]. Excess width is accommodated in a sinusoidal shape. Then the web may form a wrinkle or crease on the roller at the end of the span, which may be a problem if the crease becomes permanently folded over, ironed-in by a nip roller or if the roller is performing another duty such as liquid coating or heat transfer.

To maintain the crease on the roller, there must be a TD compressive stress σ_y in the web at the crease exceeding the critical value for buckling [33]. The critical value σ_{crit} is much higher on the roller than in the free span, so troughing may appear without creasing on the roller. The compressive stress is zero at the edges of the web width w, and rises towards the web centre with a gradient determined by traction as shown in figure 10. A crease can form if:

$$\sigma_{y\,max} = \frac{\mu_T T w}{2Rt} > \sigma_{crit} = \frac{0.605 Et}{R} \qquad \{12\}$$

Experimental data on wrinkling caused by an inclined roller are consistent with equation {12} [34]. For a given angle, wrinkles do not form below a certain tension, which is higher at greater web speed due to lower coefficient of traction.

Common observations of creasing can easily be explained. They do not occur at the edges of the web, because the TD stress there is too small. They disappear as machine speed is increased, because the coefficient of traction falls. They can also be removed from a particular roll by introducing a speed mismatch, so more of the available traction produces an MD tension and the TD stress cannot become large enough to form a crease.

Another form of wrinkling can sometimes be seen in thin films on smooth rollers at high speed. The web forms a regular sinusoidal shape in the TD, with the peaks and troughs running around the roller circumference. The wavelength is much smaller than that in the free spans. This is the buckling mode expected for a thin cylindrical shell [33]. The web is in the floating condition with an air layer of tens of microns. The shape may develop until the troughs contact the roller surface, when they are deep enough to be seen. If web-roller contact does occur, there may be small amount of traction, which would not otherwise be expected.

Lateral Contraction and Scratching

If web tension changes whilst passing over a roller, there will be an accompanying width change as a result of Poisson's ratio expansion or contraction. This will occur partly on the roller, and may result in scratches. A finite element model [27] can predict slip paths during the contact, which will generate scratches from debris or large asperities. The results shown in figure 11 demonstrate that at the web centre line slip occurs only in the MD. Nearer the edge, the slip path orientation moves towards the TD and the overall length increases. The microslip zone occupies a greater proportion of the angle of wrap at the edge.

INELASTIC EFFECTS

Real webs may be very different from the elastic ones assumed in previous sections. When held at constant length, the tension of an elastic web does not change. However,

the tension of a real web may decrease with time due to stress relaxation, a temperature rise or increase in moisture content. (Tension increases are also possible from these mechanisms and from residual shrinkage.)

In a stick zone on a roller, therefore, the web does not change length but may change tension. However, the maximum rate of tension change is still limited by traction as in equation {8}. If the rate of tension change at constant length exceeds this, the web must slide and either extend or contract so that {8} is obeyed. This may lead to the appearance of microslip zones at any location along the contact where the rate of tension change is high. For a viscoelastic web, this would normally be at the entry [35]. The exit microslip zone will also be modified in extent. Predicted curves of tension around the wrap for high and low traction are shown in figure 12.

As a consequence, the web may be moving relative to the roll surface over part of or the entire wrap, even if the entry and exit tensions are equal. Although the tension ratio is still limited by equation {6}, the relative movement of the web over the roller may be much larger than in the elastic case. This factor, together with the increased susceptibility to damage of viscoelastic, hot or wet webs, may lead to scratching problems.

Model of Vacuum Coater

A number of the effects described in this review were significant for a wrinkling problem in a vacuum coater. In this application, a 12 μm layer of metal was deposited on a 25 μm thick, 0.4 m wide PTFE film by vacuum evaporation at 0.1 m/s. The film was nipped on entry against a 0.6 m diameter drum cooled to -30 deg C. After 60 deg wrap, the web was exposed to the source for 154 deg, and then cooled over the final 38 deg. The web was prone to form wrinkles on the drum in the machine direction. They lifted the web from the drum surface, diminishing the cooling effect and allowing the vapour condensation and radiation to heat up the wrinkles, setting them in and damaging the product.

The process was modelled [36] by setting up difference equations using Mathcad [37] to understand the effect of process variables and find operating conditions to prevent wrinkling. The program followed temperature, MD tension, MD strain, distance travelled and material deposited around the drum. The MD tension changes were driven by thermal expansion, residual shrinkage and freezing-in of strain on cooling. The material response depended on the traction behaviour: a friction coefficient of 0.2 was used. The initial value of transverse elastic strain was set at the maximum the entry tension would support (equation {12}), as there was a bow roller prior to the touchdown nip. The transverse elastic strain was calculated around the drum by combining thermal expansion and Poisson's ratio effects from changes in MD elastic and frozen-in strains, assuming constant width throughout. Wrinkling was assumed to occur if the transverse strain became negative (i.e. compressive), as the critical buckling stress was low.

Figure 13 shows the variation of tension around the drum for an entry tension of 68 N and exit tensions of 50 and 126 N. In the first case (a), the tension falls over the initial 0.5 m of contact. Although the heating only commences at 0.3 m, the microslip zone appears to extend right back to the start of the contact. The tension remains just below 60 N through most of the hot zone, and then falls to the exit value over the last part of the contact, even though the thermal contraction is attempting to increase the tension. With a higher exit tension in case (b), the tension increases over the exit microslip zone, which now extends back to around 0.5 m. The two cases do not coincide over the first part of the contact: this is due to the friction algorithm used and is probably unrealistic.

199

Figure 14 shows the predicted transverse elastic strains for the two cases. The initial increase is due to the web cooling from ambient to –30 deg C. Once the web enters the hot zone, the strain falls as a result of thermal expansion and becomes compressive in case (a). The web would wrinkle in this region. Even though the strain reverts to tensile later, the damage will have been done. On the other hand, in case (b) with high exit tension, the microslip zone intervenes before the strain can become compressive. The strain set up by the MD tension increase overcomes the thermal expansion. This strain increase continues through to the web exit, and in reality would probably cause some width reduction.

The model demonstrates that increasing exit tension can reduce wrinkling, by increasing the size of the exit microslip zone back into the region where the TD elastic strain would otherwise become compressive. It also enables the effect of varying material properties, such as thermal expansion coefficient and residual shrinkage, to be studied.

CONCLUDING REMARKS

Traction can influence the behaviour of webs in process equipment in several ways. Some, such as wrinkling and scratching, can damage the web. Others, such as uncontrolled lateral movement, can limit productivity through limiting the usable web width and operating speeds. Understanding exists, and models can be developed, based on the "coefficient of traction", which enable the problems to be addressed and suitable solutions implemented. These may be changes in the surfaces, machine configuration or operating conditions. In some cases, the models are simple formulae, which can be implemented using a calculator, spreadsheet or software program [11]. In other cases, such as the tension through the machine and the vacuum coater, a computer program is needed to work through the logic and solve the coupled equations. Where stress and strain at all points on the web are needed, a stress analysis program such as Finite Elements is required, at considerably greater expense.

The coefficient of traction is itself an approximation to the real behaviour, although it is useful to envisage and apply. There is scope for further improvement in accuracy by relating it to fundamental models of surface contact, and choosing appropriate surface characterisation parameters. The web on a roller contact may also have regions of enhanced contact at the exit and edges: their effect should be better quantified.

ACKNOWLEDGEMENT

REFERENCES

1.   Whitworth, D. P. D. and Harrison, M. C., "Tension Variations in Pliable Material in Production Machinery," Appl. Math. Modelling, Vol. 7, June 1983, pp. 189-196.
2.   Daly, D. A., "Factors Controlling Traction Between Webs And Their Carrying Rollers," TAPPI Journal, Vol. 48, No. 9, Sep. 1965, pp. 88-90.
3.   Knox, K. L. and Sweeney, T. L., "Fluid Effects Associated with Web Handling," Ind. Eng. Chem. Process Des. Develop., Vol. 10, No. 2, 1971, pp. 201-206.
4.   Blok, H. and van Rossum, J. J., Lubric. Eng., Vol. 9, 1953, pp. 316 ff.

5. Eshel, A. and Elrod, H. G., "The Theory of the Infinitely Wide, Perfectly Flexible, Self-Acting Foil Bearing," ASME Journal of Basic Engineering, Vol. 87, No. 4, Dec. 1965, pp. 831-836.

6. Jones, D. P., "Air Entrainment as a Mechanism for Low Traction on Rollers and Poor Stacking of Polyester Film Reels, and its Reduction," ASME Special Publication no. AMD-149, "Web Handling 1992," ed. J.K. Good, pp. 123-131.

7. Ducotey, K. S. and Good, J. K., "The Importance of Traction in Web Handling," ASME Journal of Tribology, Vol. 117, 1995, pp. 679-684.

8. Ducotey, K. S. and Good, J. K., "Predicting Traction in Web Handling," ASME Journal of Tribology, Vol. 121, Jul. 1999, pp. 618-624.

9. Forrest, A. W., Bennett, A. N. and Jones, M. R., "Differentially Driven S-Wrap Rolls for Improved Tension Isolation," Proceedings of the Fourth International Conference on Web Handling. Ed. Good, J. K., Oklahoma State University, 1997, pp. 341-354.

10. "Traction", available to sponsors of the Web Handling Research Center, Oklahoma State University, Stillwater, OK 74078, USA.

11. "TopWeb", by Rheologic Ltd, PO Box 28, Leeds, LS8 1UH, UK.

12. Forrest, A. W. and Anderson, V. L., "Film Surface Considerations for Enhanced Winding of Thin Films," Proceedings of the Fourth International Conference on Web Handling. Ed. Good, J. K., Oklahoma State University, 1997, pp. 44-57.

13. Wu, Y. and Talke, F. E., "The Effect of Surface Roughness on the Head-Tape Interface," ASME Journal of Tribology, Vol. 118, April 1996, pp. 376-381.

14. Schüler, D., Welp, E.G. and Kopp, O., "Closed Solid-State Mechanical Model for Calculating the Transferable Torque on Wrapped Rolls," Proceedings of the Fifth International Conference on Web Handling. Ed. Good, J. K., Oklahoma State University, 1999, pp. 623-638.

15. Greenwood, J. A. and Williamson, J. B. P., "Contact of Nominally Flat Surfaces," Proc. Roy. Soc. London, Series A, Vol. 295, 1966, pp. 300-319.

16. Rice, B. S., Cole, K. A. and Müftü, S., "An Experimental and Theoretical Study of Web Traction over a Nonvented Roller," Proceedings of the Fifth International Conference on Web Handling. Ed. Good, J. K., Oklahoma State University, 1999, pp. 583-606.

17. Johnson, K. L., Contact Mechanics, Cambridge University Press, Cambridge, 1985.

18. Forrest, A. W., "A Mathematical and Experimental Investigation of the Stack Compression of Rough Films," Proceedings of the Second International Conference on Web Handling. Ed. Good, J. K., Oklahoma State University, 1993, pp. 191-206.

19. Burgdorfer, A., "The Influence of the Molecular Mean Free Path on the Performance of Hydrodynamic Gas Lubricated Bearings," ASME Journal of Basic Engineering, March 1959, pp. 94-100.

20. Bhushan, B. and Tonder, K., "Roughness-Induced Shear- and Squeeze-Film Effects in Magnetic Recording – Part II: Applications," ASME Journal of Tribology, Vol. 111, April 1989, pp. 228-237.

21. Eshel, A., "On Fluid Inertia Effects in Infinitely Wide Foil Bearings," ASME Journal of Lubrication Technology, Jul. 1970, pp. 490-494.

22. Müftü, S. and Benson, R. C., "Modelling the Transport of Paper Webs Including the Paper Permeability Effects," Advances in Information Storage and Processing Systems, ASME Int. Mech. Eng. Congress and Exposition, San Francisco, CA., ISPS-Vol. 1, 1995, pp. 247-258.

23. Licht, L., "An Experimental Study of Elastohydrodynamic Lubrication of Foil Bearings," ASME Journal of Lubrication Technology, Vol. 30, Jan. 1968, pp. 199-220.

24. Ries, J. P. and Farr, T. J., "Experimental Study of Idler Roll Slippage," Proceedings of the Fifth International Conference on Web Handling. Ed. Good, J. K., Oklahoma State University, 1999, pp. 607-621.

25. Hashimoto, H., "Improvement of Web Spacing Characteristics by Two Types of Guide Rollers", Proceedings of the Fifth International Conference on Web Handling. Ed. Good, J. K., Oklahoma State University, 1999, pp. 561-581.

26. TAPPI Journal, Dec. 1986, p 47 ff. This instrument was made by C-AN AS, Norway.

27. Zahlan, N. and Jones, D. P., "Modelling Web Traction on Rollers," Proceedings of the Third International Conference on Web Handling. Ed. Good, J. K., Oklahoma State University, 1995, pp. 156-171.

28. Shelton, J. J. and Reid, K. N., "Lateral Dynamics of a Real Moving Web," ASME Journal of Dynamic Systems, Measurement and Control, Vol. 93, No. 3, 197, pp. 180-186.

29. Young, G. E., Shelton, J. J. and Fang, B., "Interaction of Web Spans: Part I, Statics," ASME Journal of Dynamic Systems, Measurement and Control, Sep. 1989.

30. Dobbs, J.N. and Kedl, D. M., "Wrinkle Dependence on Web Roller Slip," Proceedings of the Third International Conference on Web Handling. Ed. Good, J. K., Oklahoma State University, 1995, pp. 366-381.

31. Good, J.K., "Shear in Multispan Web Systems", Proceedings of the Fourth International Conference on Web Handling. Ed. Good, J. K., Oklahoma State University, 1997, pp. 264-286.

32. Gehlbach, L. S., Good, L. K. and Kedl, D. M., "Prediction of Shear Wrinkles in Web Spans," TAPPI Journal, Vol. 72, No. 8, 1989.

33. Shelton J. J., "Buckling of Webs from Lateral Compressive Forces," Proceedings of the Second International Conference on Web Handling. Ed. Good, J. K., Oklahoma State University, 1993.

34. Good, J. K., Kedl, D. M. and Shelton, J. J., "Shear Wrinkling in Isolated Spans," Proceedings of the Fourth International Conference on Web Handling. Ed. Good, J. K., Oklahoma State University, 1997, pp. 462-480.

35. Whitworth, D. P. D., "Tension Variations in Pliable Material in Production Machinery," Ph. D. Thesis, University of Loughborough, UK, 1980.

36. McCann, M. J. and Jones, D. P., "Web Coating Dynamic Thermal and Wrinkling Model," Society of Vacuum Coaters 41st Annual Technical Conference, 1998, Paper W-17

37. Mathcad 7 Professional, from MathSoft Inc., 101 Main Street, Cambridge, MA, USA.
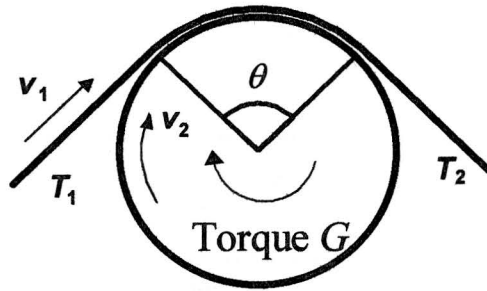
Fig. 1 Definition of quantities for web passing over a roller.
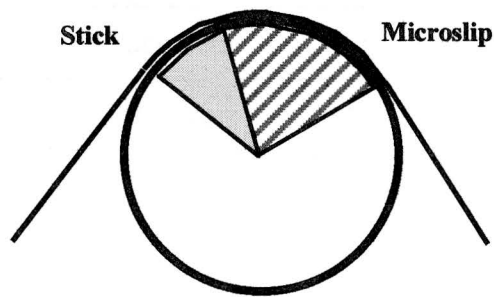
Fig. 2 Location of stick and microslip zones in steady state contact.
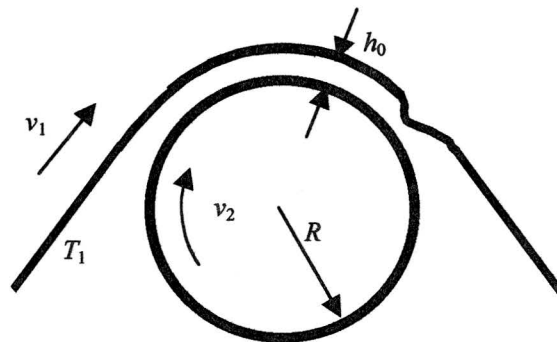
Fig. 3 Schematic diagram of air entrainment by web on a roller, showing the entry region, constant gap region and constriction in the exit region as predicted by foil bearing theory.
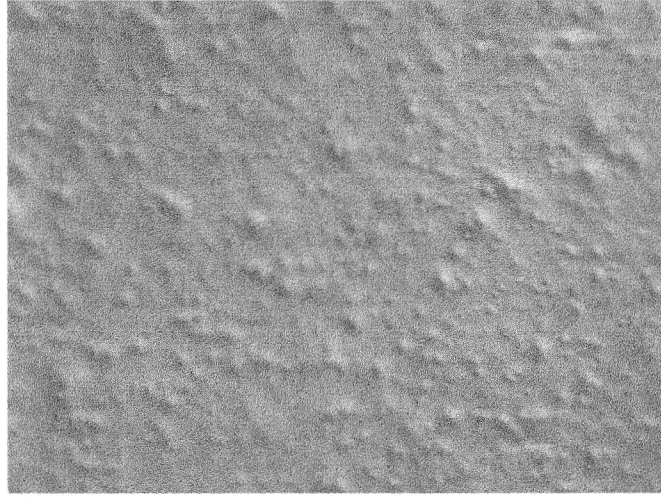
Fig. 4 Differential Interference Contrast Micrograph of a filled polyester film surface, showing surface peaks produced by inorganic particles in the bulk. The area shown is 450 μm across.
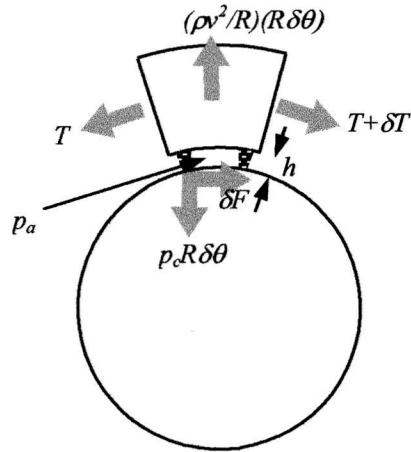
Fig. 5 Schematic diagram of forces acting on a web element. The inward resultant of tension balances the air pressure p_a, the contact pressure p_c and centrifugal force acting on the element $R\delta\theta$. If slip occurs, the friction force δF is equal to the change in tension δT.
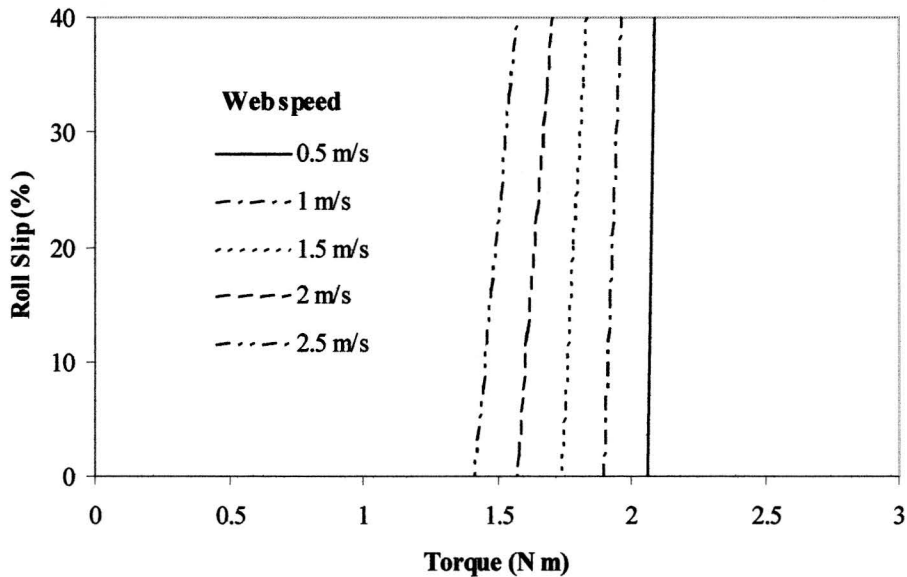
Fig. 6 Results of a simulation of the experiment of Ries and Farr [24, figure 6], to measure the percentage difference between web speed and roller speed as a function of braking torque at the web speeds shown. Roller roughness is 60 AA (1.5 μm), tension 350 N/m, wrap angle 60 deg.
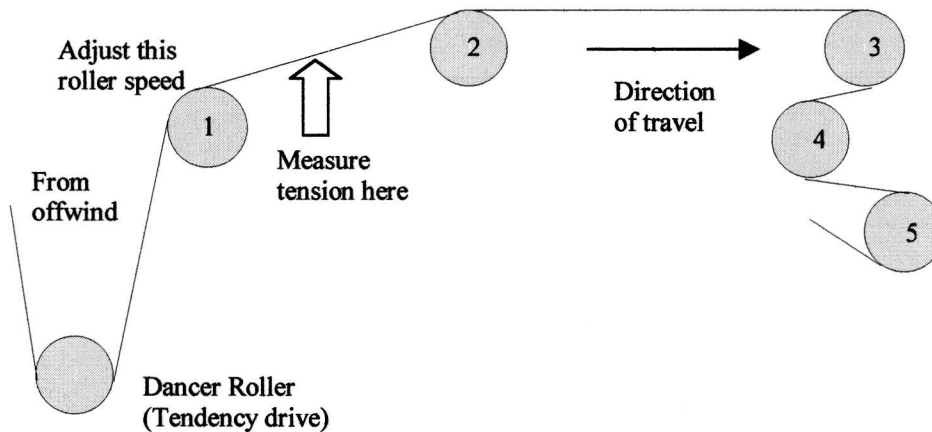
Fig. 7 Schematic partial web path through the slitter-rewinder as described in the text, showing locations of roller speed adjustment (no. 1) and tension measurement. All rollers except the dancer are speed controlled.
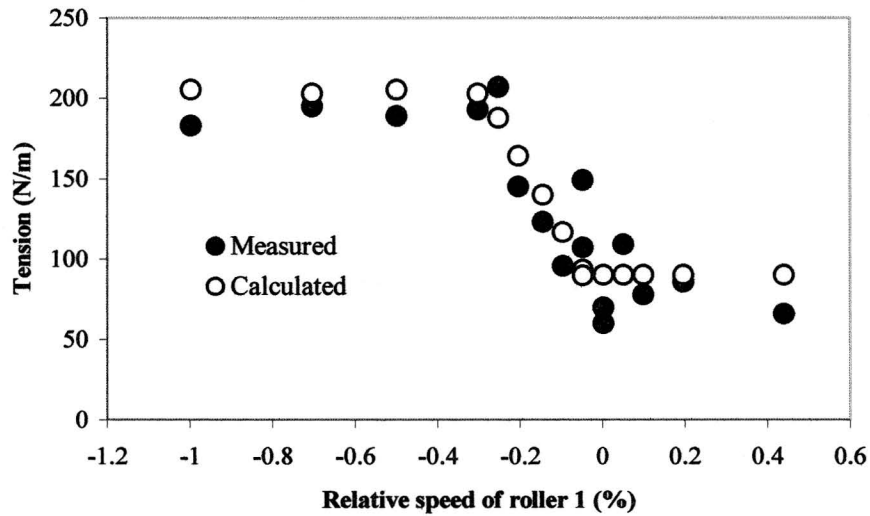
Fig. 8 Web tension at different settings of Roller 1 speed for the slitter-rewinder shown in fig. 7 at 0.5 m/s. Solid circles – measured using Tensor. Hollow circles – calculated using model described in the text.
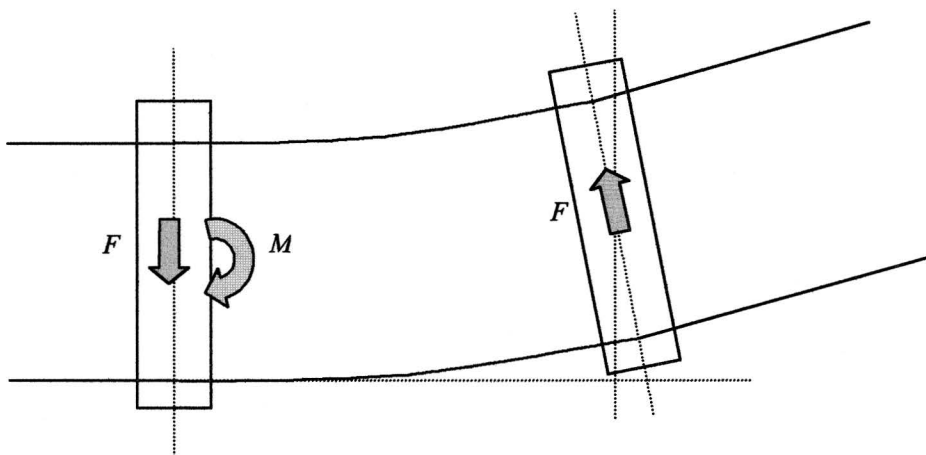
Fig. 9 Web steering produced by an inclined roller. Reaction forces F and a bending moment M are set up as shown.

(a) Web just taut

(b) Troughs in free span

(c) Crease on a roller

Compressive
Stress

Buckling
stress

creases

(d) Schematic variation of TD compressive stress, showing creases
able to form where it exceeds the critical buckling stress
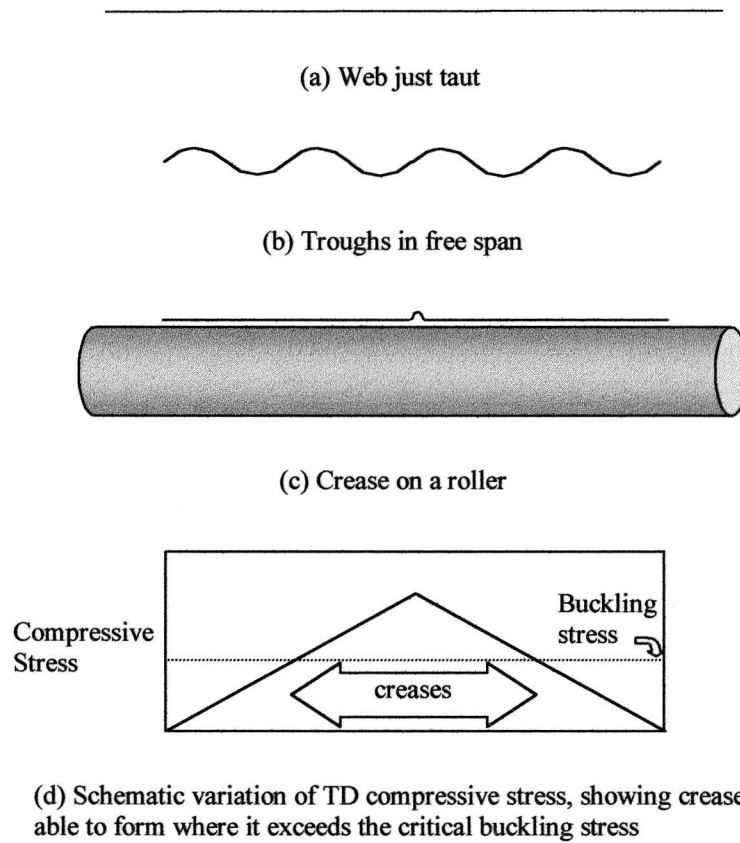
Fig. 10 Condition of a web in section, showing (a) flat, (b) troughing between rollers, (c)
creasing on a roller and (d) the compressive stress varation which produces creases in the
region shown.

MD
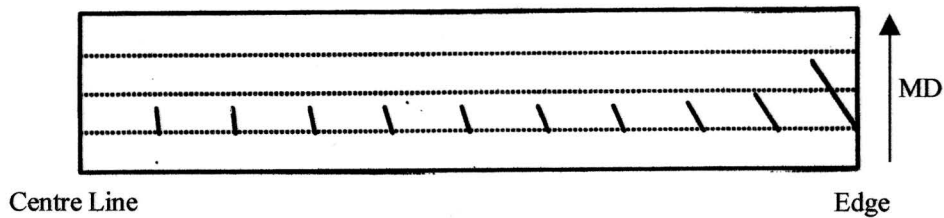
Centre Line   Edge

Fig. 11 Slip paths of web against a roller at different locations along the TD from the
centre line to the web edge, calculated using Finite Element Analysis [27]. The lengths
are magnified, with the dotted lines representing 0.5 mm.
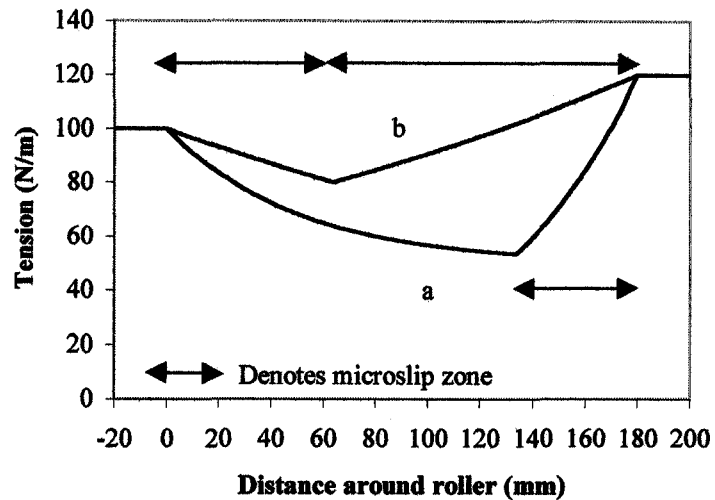
Fig. 12 Schematic variation of tension in a viscoelastic web around a roller with a braking torque applied. The indicated regions are microslip zones.

(a) Coefficient of traction = 1. Traction can support the viscoelastic decay of tension from the entry. Tension rises, and the film stretches, in the microslip zone prior to exit.

(b) Coefficient of traction = 0.2. There is a microslip zone at the entry, where the web stretches as the tension falls at a lower rate than the viscoelastic decay. There is a large microslip zone prior to exit, and a very small region of stick between the two microslip zones.
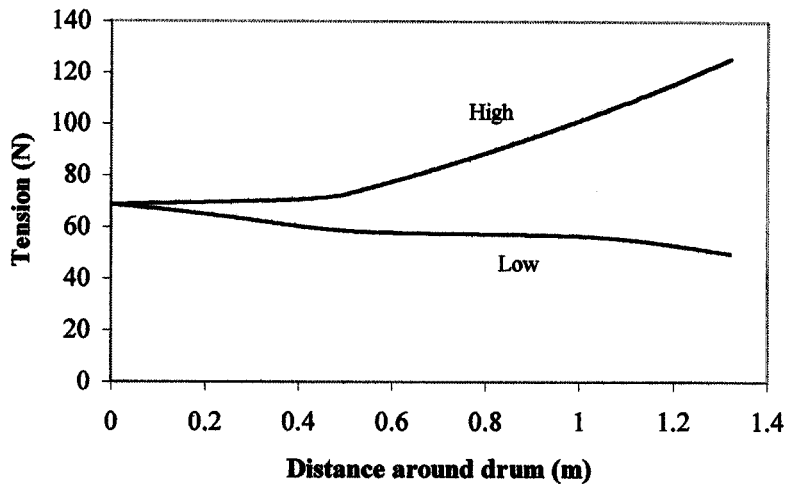
Fig. 13 Calculated tension around the vacuum coater drum for low and high exit tensions.
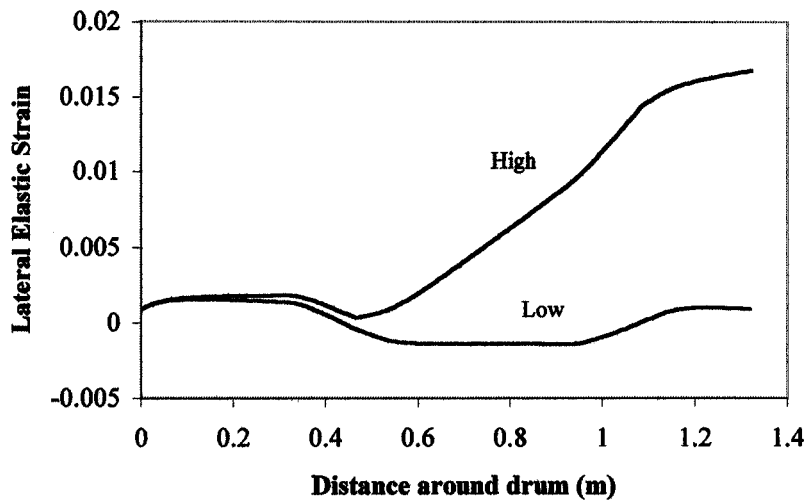
Fig. 14 Calculated tensile lateral elastic strain around the vacuum coater drum for low and high exit tension, while held at the initial width.

Name & Affiliation	Question
J. Shelton – OSU	I have never seen information on friction versus velocity for the very low velocities that could be associated with the micro-slip between webs and rollers. The static coefficient of friction is associated a maximum frictional force and the kinetic coefficient of friction is measured at a reference velocity established by testing groups such as ASTM. Are you aware of any studies that have been done in which friction has been studied as a function of slip velocity?
Name & Affiliation	**Answer**
D. Jones – Emral Ltd.	I believe there has been some work done in this area. David Tabor, who is now retired out of Cambridge, has done work in this area. Brian Briscoe, who is at the Imperial College in London, has measured friction in polymer systems. They tested some slow sliding speeds and studied friction over a large range, and I guess some of those would have encompassed web handling speeds. To my knowledge they haven't extended their work to incorporate entrained air which is the issue in web handling.
Name & Affiliation	**Question**
J. Dobbs – 3M	Can you comment more on scratching when you have micro-slip?
Name & Affiliation	**Answer**
D. Jones –Emral Ltd.	It wasn't normally a problem, but I think it can be sometimes. In my talk, I passed over this slide which was presented in my 1995 IWEB paper. This is an finite element model of web passing over a roll with a tension increase. The slide shows contours of MD tension. As you can see, there is a slip zone over the last part of contact and it is larger at the edges. In Figure 11 of this paper we traced the relative movement of the points that initially came into contact and then moved a slight distance away during contact. This shows the slip paths, shown exaggerated of course, with these dotted lines 0.5 mm apart. So this would be the typical movement distance in microslip. You can see here at the edge their length has increased and also they are much more inclined away from the machine direction. This would yield short scratches, 1 mm across the web at this point. Movement can abrade the material so it may be a debris generation source. Once those debris particles are present, or there are asperities on the roll, they can dig in and cause the scratching. So it can be a problem, but I think scratches generated by this mechanism are much less prominent than those from general slip and a speed mismatch.